THE JOURNAL OF BIOLOGICAL CHEMISTRY VOL. 291, NO. 21, pp. 11323–11336, May 20, 2016

Regulation of Cell Wall Plasticity by Nucleotide Metabolism in *Lactococcus lactis*[*]

Received for publication, January 18, 2016, and in revised form, March 16, 2016 Published, JBC Papers in Press, March 28, 2016, DOI 10.1074/jbc.M116.714303

Ana Solopova[‡], Cécile Formosa-Dague[§1], Pascal Courtin[¶], Sylviane Furlan[¶], Patrick Veiga[¶2], Christine Péchoux[‖], Julija Armalyte[¶3], Mikas Sadauskas[¶4], Jan Kok[‡], Pascal Hols[§5], Yves F. Dufrêne[§6], Oscar P. Kuipers[‡], Marie-Pierre Chapot-Chartier[¶], and Saulius Kulakauskas[¶7]

From the [‡]Department of Molecular Genetics, Groningen Biomolecular Sciences and Biotechnology Institute, University of Groningen, Nijenborgh 7, 9747AG Groningen, The Netherlands, [§]Institute of Life Sciences, Université catholique de Louvain, Croix du Sud 4-5, bte L7.07.06., B-1348 Louvain-la-Neuve, Belgium, and [¶]Micalis Institute and [‖]Génétique Animale et Biologie Intégrative, Institut National de la Recherche Agronomique, AgroParisTech, Université Paris-Saclay, 78350 Jouy-en-Josas, France

To ensure optimal cell growth and separation and to adapt to environmental parameters, bacteria have to maintain a balance between cell wall (CW) rigidity and flexibility. This can be achieved by a concerted action of peptidoglycan (PG) hydrolases and PG-synthesizing/modifying enzymes. In a search for new regulatory mechanisms responsible for the maintenance of this equilibrium in *Lactococcus lactis*, we isolated mutants that are resistant to the PG hydrolase lysozyme. We found that 14% of the causative mutations were mapped in the *guaA* gene, the product of which is involved in purine metabolism. Genetic and transcriptional analyses combined with PG structure determination of the *guaA* mutant enabled us to reveal the pivotal role of the *pyrB* gene in the regulation of CW rigidity. Our results indicate that conversion of L-aspartate (L-Asp) to *N*-carbamoyl-L-aspartate by PyrB may reduce the amount of L-Asp available for PG synthesis and thus cause the appearance of Asp/Asn-less stem peptides in PG. Such stem peptides do not form PG cross-bridges, resulting in a decrease in PG cross-linking and, consequently, reduced PG thickness and rigidity. We hypothesize that the concurrent utilization of L-Asp for pyrimidine and PG synthesis may be part of the regulatory scheme, ensuring CW flexibility during exponential growth and rigidity in stationary phase. The fact that L-Asp availability is dependent on nucleotide metabolism, which is tightly regulated in accordance with the growth rate, provides *L. lactis* cells the means to ensure optimal CW plasticity without the need to control the expression of PG synthesis genes.

Peptidoglycan (PG)[8] is the major component of the Gram-positive bacterial cell wall (CW), which envelops the cell as a multilayer sacculus. PG consists of a basic unit made up of *N*-acetylglucosamine-*N*-acetylmuramic acid (GlcNAc-MurNAc) disaccharides bound to stem pentapeptides. Disaccharide pentapeptide units are synthesized intracellularly and transported through the cytoplasmic membrane as lipid-disaccharide pentapeptides called lipid II. These blocks are covalently linked to the pre-existing PG polymers by high molecular weight penicillin-binding proteins (PBPs) (1). Class A PBPs contain both transglycosylation and transpeptidation domains, whereas class B PBPs are involved only in transpeptidation. Transglycosylation links the disaccharide pentapeptide to the pre-existing PG chain, whereas transpeptidation connects the stem pentapeptides to neighboring chains, which ensures PG cross-linking through the formation of an interpeptide bridge. Cross-linking in *Lactococcus lactis* involves the synthesis of an interpeptide bridge made of one D-amino acid (D-Asp or D-Asn), and in this species the PG cross-linking index was estimated to be 35.5% (2). Studies of *Staphylococcus aureus* have revealed that this PG cross-linking correlates with CW rigidity (3).

The basic PG structure is often modified as PG glycan chains can undergo *N*-deacetylation or *O*-acetylation, and free carboxyl groups of amino acids of peptide chains may be amidated (4). In *L. lactis*, MurNAc *O*-acetylase is encoded by the *oatA* gene and is associated with resistance to peptidoglycan hydrolases (PGHs) (5). *N*-Deacetylation of the GlcNAc present in PG is achieved by the PG deacetylase PgdA and has also been shown to protect PG from PGH activity (6, 7). The free carboxyl groups of PG-forming amino acids are amidated intracellularly before the precursors are translocated through the cytoplasmic membrane (8). In *L. lactis*, these amino acids include D-Glu found in stem peptides and D-Asp on side chains or cross-bridges (2). Amidation of D-Asp takes place after it has been added to the PG precursor by AslA and is catalyzed by an asparagine synthase (AsnH) (9) because D-Asn is not a substrate for the aspartate ligase AslA (10). In *L. lactis*, the D-Asp cross-bridge is only partially (75%) amidated during the exponential phase in contrast to other bacteria in which amidation is almost

* This work was supported in part by the Institut National de la Recherche Agronomique and the Région Ile-de-France (to P. C., S. F., P. V., J. A., M. S., M.-P. C.-C., and S. K.) and the National Foundation for Scientific Research (FNRS) and the Research Department of the Communauté française de Belgique (Concerted Research Action) (to C. F.-D., Y. F. D., and P. H.). The authors declare that they have no conflicts of interest with the contents of this article.

[1] Postdoctoral researcher at FNRS.
[2] Present address: Danone Nutricia Research, RD 128, avenue de la Vauve, F-91767 Palaiseau, France.
[3] Recipient of a fellowship from the Région Ile-de-France (Domaine d'Intérêt Majeur Malinf). Present address: Dept. of Biochemistry and Molecular Biology, Faculty of Natural Sciences, Vilnius University, M. K. Čiurlionio 21, LT-03101 Vilnius, Lithuania.
[4] Present address: Dept. of Microbiology and Biotechnology, Faculty of Natural Sciences, Vilnius University, Čiurlionio 21/27, 03101 Vilnius, Lithuania.
[5] Senior research associate at FNRS.
[6] Research director at FNRS.
[7] To whom correspondence should be addressed. Tel.: 33-1-34-65-2073; Fax: 33-1-34-65-20-65; E-mail: Saulius.Kulakauskas@jouy.inra.fr.

[8] The abbreviations used are: PG, peptidoglycan; PGH, peptidoglycan hydrolase; CW, cell wall; PBP, penicillin-binding protein; GlcNAc, *N*-acetylglucosamine; MurNAc, *N*-acetylmuramic acid.

complete (2). D-Asp amidation of *L. lactis* PG decreases sensitivity to cationic antimicrobials, such as lysozyme or nisin, which may be related to a reduction of the net negative charge inside the cell wall (10).

A strong PG sacculus is needed to counteract both high turgor pressure and cell wall stress related to environmental factors. At the same time, cleavage of PG strands is needed to allow the insertion of newly synthesized PG blocks during bacterial cell growth and for daughter cell separation after division (2, 11, 12). PG flexibility is especially advantageous during exponential growth. Two opposing features of PG, *i.e.* rigidity and flexibility, require the coordinated and balanced action of PG-synthesizing and degradation enzymes. The loss of this balance may cause growth arrest and/or cell lysis. In bacteria, such a balance is achieved mostly by regulating the activities of potentially lethal autolytic enzymes, such as PGHs (13). The factors that affect CW sensitivity to autolysins include (i) their proteolytic degradation (14); (ii) their specific localization within the cell, often at the septal region; (iii) shielding of PG from PGH by secondary cell wall polymers, such as teichoic acids or wall polysaccharides; (iv) alanylation of (lipo)teichoic acids; (v) *O*-acetylation or *N*-deacetylation of PG; (vi) amidation of D-Glu and D-Asp in PG stem peptides; and (vii) glycosylation of autolysins (2). In addition to the introduction of PG breaks by PGHs, PG flexibility in *L. lactis* could also result from defective PG synthesis and cross-linking due to a deficiency in PonA, one of the class A PBPs (15). PG plasticity could also be enhanced by the incorporation of exogenously added non-canonical D-amino acids into PG (16). For example, the weakening of CWs by incorporation of the achiral amino acid glycine is exploited for the preparation of competent cells of Gram-positive bacteria (17, 18).

It is important to note that too rigid PG also has deleterious consequences for bacterial growth. Overexpression of the *L. lactis oatA* gene leads to PG that is excessively resistant to PGH and consequently results in growth arrest (7). The lethal effect of overly strong PG is consistent with findings that several PGHs are collectively essential for the growth of *Escherichia coli*, *Bacillus subtilis*, and *Staphylococcus aureus.* This lethality could be related to the need for PGH-mediated PG remodeling during key steps in the cell cycle (19–22).

To identify factors that may be involved in maintenance of the balance between CW flexibility and CW rigidity during cell growth, we isolated mutants of *L. lactis* that were resistant to hen egg white lysozyme. Analysis of one class of resistant mutants, which had a deletion of a large chromosome fragment encompassing the *guaA* gene, led us to the potential mechanism that allows the adjustment of CW rigidity to bacterial growth rate requirements without the transcriptional regulation of gene expression. This mechanism is based on the utilization of L-Asp for both PG and pyrimidine synthesis. To the best of our knowledge, the presented data are the first indication of a link between nucleotide metabolism and cell wall plasticity in bacteria.

Experimental Procedures

Bacterial Strains and Growth Conditions—The bacterial strains and plasmids used in this study are listed in Table 1. All *L. lactis* strains used here are derivatives of strain MG1363 (23). *L. lactis* was grown at 30 °C in M17 medium (BD Biosciences) that contained 0.5% glucose (M17G). Erythromycin (2.5 μg/ml) and chloramphenicol (5 μg/ml) (Sigma) were added when needed. *E. coli* was grown in LB medium (BD Biosciences) at 37 °C, unless otherwise indicated, in the presence of ampicillin (100 μg/ml), erythromycin (100 μg/ml), or chloramphenicol (10 μg/ml) when needed. Nisin was prepared in Me_2SO (Sigma) and added at a final concentration of 0.1 ng/ml. Growth was monitored by absorbance measurement at 600 nm (A_{600}) with a spectrophotometer (Spectronic 20 Genesys).

Lysozyme Resistance Tests—A concentrated hen egg white lysozyme (Fluka, Buchs, Switzerland) solution was freshly prepared in M17G medium and then diluted in molten M17G agar (1.5%) at 45 °C. Overnight bacterial cultures were successively diluted 10-fold, and 5 μl of each dilution was spotted on M17G agar plates supplemented with different concentrations of lysozyme.

Strain Constructions—A 1347-bp fragment containing the *guaA* gene was deleted from the chromosome using the pORI280 (*lacZ*$^+$)/pVE6007 two-plasmid system (24, 25). First, the fragments upstream (578 bp) and downstream (607 bp) of the deletion site were PCR-amplified from *L. lactis* MG1363 genomic DNA using primer pairs guaA-bgl (5′-atgatgagatcttcaagctttctacattgcc; restriction site is underlined) and guaA-xmab (5′-atgatgcccgggatgagttctgagaaaacacc) and primer pairs guaA-xmax (5′-atgatgcccgggaaaacgtatcgtcaatgagg) and guaA-xba (5′-atgatgtctagacatctccaataaacatctgg). Then both fragments were digested with the restriction endonuclease SmaI (New England Biolabs) and PCR-amplified using primers guaA-bgl and guaA-xba. The amplified region was digested with BglII and XbaI and ligated with T4DNA ligase (New England Biolabs) to a BglII-XbaI-digested pORI280, and the ligation mixture was used to transform *E. coli* JIM4646. The pORI280 derivative that was needed for construction of a *guaA* deletion mutant was obtained as an erythromycin-resistant transformant. The resulting plasmid, pVES4848, and a thermosensitive plasmid encoding chloramphenicol resistance, pVE6007, were introduced into MG1363; transformants were selected by erythromycin (2.5 μg/ml) and chloramphenicol (2.5 μg/ml) resistance. Plasmid pVES4848 was integrated in the resulting strain following overnight growth in erythromycin-supplemented M17G liquid medium at 37 °C, a temperature that prevents pVE6007 replication. The culture was then plated on M17G agar with erythromycin, and four independent chloramphenicol-sensitive clones were isolated and grown on M17G without antibiotics for at least 100 generations. Strain VES4883 (Δ*guaA*) was then selected as a white colony on M17G agar supplemented with X-gal (5-bromo-4-chloro-3-indolyl-β-D-galactopyranoside; Euromedex, Souffelweyersheim, France) and verified by PCR and nucleotide sequence determination. To inactivate the *pyrB* gene, we followed the same procedure using the primer pairs pyrBBglII (5′-tgttgtagatctcgatttatgtgattgctgg) and pyrBXmaR (5′-tgttgtcccgggaaggtctcctttaccctg) for amplification of the upstream 588-bp fragment and pyrBXmaF (5′-tgttgtcccgggatggccattcttgaagcc) and pyrBXbaI (5′-tgttgttctagacagtagcttgaagttggc) for the downstream 576-bp fragment.

The resulting strain, VES6497, carried a deletion of the 888-bp fragment that contained *pyrB*.

Similarly, the *guaA* deletion was introduced in strain VEL1378 (*dltD*), creating strain VES5160, and the *pyrB* deletion was introduced in strain VES4883 (Δ*guaA*), yielding VES6530. Also, the Δ*acmA* mutation was introduced in strain VES6497 by using the plasmid pINTAA and following the procedure described previously (14), thus creating strain VES6831. The *ponA pyrB* double mutant VES6949 was constructed by transforming strain VES6497 with plasmid pVE1837 (pRV300 carrying a 210-bp internal fragment of *ponA* (26)) and selecting for erythromycin resistance.

Mapping of Spontaneous guaA Mutation—With primers gua1 (5′-cggacttttgcaccttataa) and gua2 (5′-gcgttaatagaattatagcg), we PCR-amplified a 1786-bp fragment of *L. lactis* MG1363 genomic DNA but were unable to obtain the corresponding DNA fragment using DNA of the mutant VES2824 (Fig. 1). However, in the latter strain, we were able to amplify a 3590-bp DNA fragment using primers gua3 (5′-tttatacgggaatcgttgcg) and gua4 (5′-ttggcacttaattcttgccc). DNA sequence determination of this fragment revealed that it contained the IS*905* transposon DNA sequence flanked by sequences that are situated upstream and downstream of IS*905* transposons, indicating that VES2824 is missing the 33,893-bp chromosomal fragment situated between the two IS*905*s.

Cloning of pyrB under Control of the Nisin-inducible Promoter—The DNA fragment carrying the *pyrB* gene was PCR-amplified from *L. lactis* MG1363 genomic DNA using the primer pair 7.gibs.pyrB1 (5′-aaataaattataaggaggcactcaccATGTCAGTAAAAAATGGATTAGTTC, nucleosides in uppercase correspond to *pyrB* gene sequence; those in lowercase are plasmid sequence) and 8.gibs.pyrB2 (5′-agtggtaccgcatgcctgcagtaccAACTTACTTCGCTTTTTTTCCAGCAAG). The fragment was ligated to the NcoI-digested plasmid pMSP3545 using isothermal assembly (27) and introduced in VES6497. The clone that carried plasmid pMSP3545::*pyrB*$^{+}$ (nisin-inducible *pyrB*), VES6953, was verified by PCR and DNA nucleotide sequence determination.

Peptidoglycan Structure Analysis—PG was extracted from cultures in the exponential (A_{600} 0.4 for MG1363 and A_{600} 0.2 for VES6497 (Δ*pyrB*) and VES4883 (Δ*guaA*)) and early stationary growth phases (A_{600} 1.2 for MG1363) as described previously (28). PG was then hydrolyzed with mutanolysin, and the resulting soluble muropeptides were reduced and separated by reverse phase HPLC with an Agilent UHPLC 1290 system using an ammonium phosphate buffer and linear methanol gradient as described previously (29). The eluted muropeptides were detected by UV absorbance at 202 nm. Muropeptides were identified according to their retention time by comparison with a reference chromatogram (28). The different muropeptides were quantified by integration of the peaks on the chromatogram. The relative amount of each muropeptide was expressed as the ratio of its peak area over the sum of all of the peak areas. The PG cross-linking index was calculated as described previously (30).

DNA Microarray Analysis—For DNA microarray experiments, *L. lactis* MG1363 and *L. lactis* VES4883 (Δ*guaA*) cells were grown in M17G medium and harvested at the midexponential growth phase. To assess the effect of the lysozyme treatment on the transcriptome, 5 mg/ml lysozyme (Sigma-Aldrich) was added to the culture. Cells were collected after 20 min of incubation with lysozyme. Total RNA of lysozyme-treated MG1363 and of VES4883 was compared with RNA isolated from MG1363 (WT) cells. Slides were scanned with a Genepix 4200 laser scanner at 10-μm resolution. ArrayPro 4.5 (Media Cybernetics Inc., Silver Spring, MD) was used to analyze slide images; processing and normalization were performed using MicroPrep software (31, 32) as described previously (32). Gene expression was considered to be significantly altered when the Cyber-T Bayesian *p* value was ≤0.001.

Transmission Electron Microscopy—Pellets of bacteria (A_{600} 0.5 for MG1363, MG1363 + uracil, and Δ*pyrB* mutant + uracil and A_{600} 0.2 for the Δ*pyrB* mutant) were fixed with 2% glutaraldehyde in 0.1 M sodium cacodylate buffer, pH 7.2, for 3 h at room temperature. Samples were contrasted with 0.5% oolong tea extract in cacodylate buffer, fixed with 1% osmium tetroxide that contained 1.5% potassium cyanoferrate, gradually dehydrated in ethanol (30–100%), substituted gradually in a mixture of propylene oxide-Epon, and embedded in Epon (Delta Microscopie, Labège, France). Thin (70-nm) sections were collected onto 200 mesh copper grids and counterstained with lead citrate. Grids were examined using a Hitachi HT7700 electron microscope operated at 80 kV (Elexience, France). Images were acquired with a charge-coupled device camera (Advanced Microscopy Techniques, Corp., Japan). Cell wall thickness was measured on transmission electron microscopy micrographs of at least three cells at magnification 70,000×, taking at least five measurements on each cell.

Sample Preparation and Atomic Force Microscopy Experiments—L. lactis strains MG1363 and its isogenic Δ*pyrB* mutant were grown in M17G broth in the presence or absence of 100 μg/ml uracil at 30 °C under static conditions until the exponential phase was reached (A_{600} 0.5 for MG1363, MG1363 + uracil, and Δ*pyrB* mutant + uracil and A_{600} 0.2 for the Δ*pyrB* mutant). Bacterial cells were concentrated by centrifugation, washed twice, resuspended in phosphate-buffered saline (PBS), and immobilized on polydimethylsiloxane stamps prepared as described previously (33). Briefly, microstructured polydimethylsiloxane stamps were covered by a total of 100 μl of the cell suspension. Cells were then deposited into the microstructures of the stamps by convective/capillary assembly.

Images were recorded in PBS in Quantitative Imaging™ (QI™) mode (34) using MSCT AUWH (Bruker, Billerica, MA) cantilevers (nominal spring constants of 0.1 and 0.01 newton/m) and an applied force of 0.5 nanonewton. Force spectroscopy mode was used to perform local nanoindentation measurements on areas of 500 × 500 nm^2 on top of cells. The applied force was kept between 0.5 and 2 nanonewtons depending on the strains and growth conditions probed. The cantilevers' spring constant was determined using the thermal noise method (35). For imaging and force spectroscopy, we used a Nanowizard III (JPK Instruments, Berlin, Germany). For rigidity measurements, the force-distance curves obtained in QI™ mode and during nanoindentation experiments were transformed into force-indentation curves by subtracting the canti-

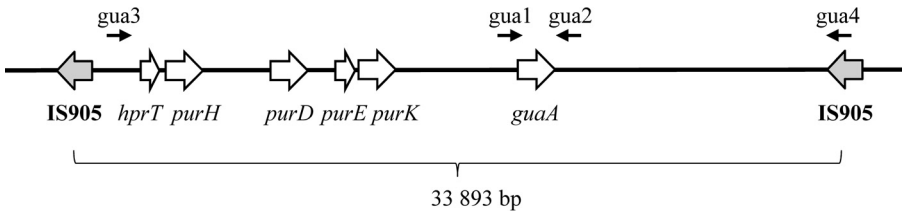

FIGURE 1. **Scheme of the *L. lactis* MG1363 chromosomal locus that contains *guaA* and other genes involved in purine metabolism.** *Black arrows* indicate the oligonucleotides used for mapping (see "Experimental Procedures").

lever deflection on a solid surface. The indentation curves were then fitted to the Hertz model, which links the force (F) as a function of the Young's modulus value (E) with the square of the indentation (δ) for a conical indenter according to the following equation: $F = [2E \tan\alpha/\pi(1 - \nu^2)]\delta^2$ where α is the tip opening angle (17.5°) and ν is the Poisson ratio, assumed to be 0.5. In each condition, the fitted indentation segment was kept constant at 50 nm. In each case, Young's modulus values were measured on 12 cells ($n = 12288$ curves per conditions), and Young's modulus medians were calculated from fits in a Gaussian model. All results were analyzed using the data processing software provided by JPK Instruments.

Results

Screening for Spontaneous Lysozyme-resistant Mutants Reveals a Deficiency in Guanine Biosynthesis—To select mutants affected in CW structure, we chose to use lysozyme for its double antibacterial activity. First, it is a muramidase and hydrolyzes the β-1,4-glycosidic bonds between *N*-acetylmuramic acid and *N*-acetylglucosamine of PG, ultimately resulting in cell lysis. Second, lysozyme acts as a cationic antimicrobial that creates pores in the cytoplasmic membrane, leading to leakage of intracellular ions from the cell (36). We reasoned that using such "bicidal" antimicrobial would allow isolation of a larger spectrum of different mutants. We selected 59 independent spontaneous lysozyme-resistant mutants of *L. lactis* strain MG1363. Of these, eight (14%) were unable to efficiently grow in rich M17G medium. This deficiency was corrected by the addition of guanine (20 μg/ml). The guanine deficiency was also confirmed using chemically defined medium (SA; Ref. 37) (results not shown). Because it has been reported that guanine auxotrophy could be due to inactivation of the *guaA* gene that encodes GMP synthase (38, 39), we verified the presence of mutations in this gene in the guanine auxotrophs. The *guaA* gene has been shown to be involved in acid resistance in *L. lactis*, a phenotype that could be linked to CW modification (39). Unexpectedly, we failed to PCR amplify the DNA fragment carrying the *guaA* gene using primers gua1 and gua2 from the chromosomal DNA of the obtained mutants (Fig. 1). In the *L. lactis* chromosome, the large 33,893-bp DNA fragment that carries the *guaA* gene is flanked by two IS*905* elements oriented in the same direction (40). This organization allows the deletion of this fragment by homologous intrachromosomal recombination. Indeed, large chromosomal rearrangements due to intrachromosomal recombination between IS*905* elements were previously shown to occur in *L. lactis* (41). We tested this possibility by PCR with primers gua3 and gua4, located outside of the IS*905* elements, and obtained a 3590-bp fragment from all eight spontaneous guanine auxotrophs. DNA nucleotide sequence determination of the amplified DNA fragment from one of these mutants, VES2824, showed that it contained one copy of IS*905* DNA, thus confirming that an intrachromosomal recombination event was the basis of the deletion. Because the deleted fragment included other genes involved in purine metabolism (Fig. 1), we constructed a deletion mutant of only the *guaA* gene (strain VES4883; Table 1). As was the case for VES2824, the mutant VES4883 required guanine for growth in M17G and SA media and exhibited identical lysozyme resistance. The lysozyme resistance of strains VES2824 and VES4883 decreased when guanine was added to the medium (Fig. 2).

*Transcriptome Analysis of the Δ*guaA* Mutant Shows Down-regulation of Pyrimidine Biosynthetic Genes*—To determine which genes may be involved in the lysozyme resistance of strain VES4883 (Δ*guaA*), we compared its transcriptional profiles with that of the control strain MG1363. To identify which genes are induced by cell wall stress, we included in this assay MG1363 cells treated with lysozyme (Table 2). In the Δ*guaA* mutant, we observed that, first, the *dlt* operon genes *dltA*, *dltB*, and *dltD*, which are responsible for D-alanylation of teichoic acids (42), were up-regulated more than 3-fold. Second, expression of *ponA*, which encodes the PG synthesis enzyme PBP1A (26), was up-regulated 4-fold in the Δ*guaA* mutant. Because this gene is involved in PG assembly, its increased expression could result in more cross-linked PG and thus contribute to lysozyme resistance. Third, expression of *pyrR*, which encodes the transcriptional regulator of the pyrimidine biosynthetic genes, was markedly decreased. This may explain the observation of strong down-regulation of other genes involved in pyrimidine biosynthesis: *pyrB*, *pyrP*, *carA*, *pyrK*, *pyrDb*, *pyrF*, *pyrE*, and *pyrC* (38). The only PG synthesis genes that were affected in the Δ*guaA* mutant were *murB* and *murC*, which encode enzymes involved in the synthesis of UDP-MurNAc pentapeptide precursors (2). Notably, the cell envelope stress genes *cesSR* and *spxB* were not up-regulated in the Δ*guaA* mutant, indicating that the lysozyme resistance of this strain is not monitored by the *cesSR* regulon.

The *cesSR* and *spxB* genes were induced in lysozyme-treated MG1363 cells as expected. This corroborated the hypothesis that lactococci react to cell wall stress by inducing genes of the *cesSR* operon, which leads to resistance to PG hydrolysis (7, 43). The expression of PG synthesis genes was not affected in lysozyme-treated cells, indicating that PG synthesis is not regulated in response to lysozyme-provoked CW stress. Despite its apparent role in lysozyme resistance, *dlt* operon expression was also not affected under these stress conditions.

TABLE 1
Strains and plasmids used in this study and their relevant genetic properties

Strains	Relevant genotype	Source/Ref.
L. lactis		
MG1363	Plasmid-free strain	23
NZ9000	MG1363 *pepN*::*nisRK*	64
VES1842	*ponA* mutant obtained by pVE1837 insertion in MG1363	26
MG1363acmAΔ1	MG1363 derivative carrying a deletion in *acmA*	14
VEL1378	MG1363 *dltD*::IS*S1*	65
VES2824	MG1363 carrying deletion of 33,893-bp chromosomal fragment containing *guaA* gene	This work
VES3787	MG1363 carrying pVES3787 (*pgdA*$^+$)	7
VES4075	MG1363 derivative carrying pVE3916	7
VES4883	MG1363 carrying deletion of *guaA*	This work
VES5160	VEL1378 (*dltD*) carrying deletion of *guaA*	This work
VES6497	MG1363 carrying deletion of *pyrB*	This work
VES6530	VES4883 (*guaA*) carrying deletions of *pyrB*	This work
VES6831	VES6497 (*pyrB*) carrying deletion *acmAΔ1*	This work
VES6949	VES6497 (*pyrB*) carrying mutation *ponA*	This work
VES6953	VES6497 (*pyrB*) carrying pMSP3545::*pyrB*$^+$ (nisin-inducible *pyrB*)	This work
VES6955	VES6497 (*pyrB*) carrying pLc-40	This work
VES6957	VES6497 (*pyrB*) carrying pMSP3545	This work
VES6959	VES6497 (*pyrB*) carrying pVE3916	This work
VES6968	MG1363 carrying pLc-P40	This work
VES6996	VES6497 (*pyrB*) carrying pVES3787 (*pgdA*$^+$)	This work
E. coli		
JIM4646	TG1 with chromosomal copy of the *repA* gene	P. Renault, Jouy-en-Josas, France
HB101	F$^-$ *mcrB mrr hsdS20 recA13 leuB6 ara-14 proA2 lacY1 galK2 xyl-5 mtl-1 rpsL20 glnV44*	66
TG1	F' *traD*36 *lacI*^{q} Δ*lacZ* (M15 *proAB*$^+$/*supE*Δ (*hsdM-mcrB*)5 *thi*Δ (*lac-proAB*)	Laboratory collection
Plasmids		
pRV300	Erythromycin-resistant pBluescript derivative	67
pVE6007	Replication-thermosensitive derivative of broad host range replicon pWV01	68
pMSP3545	Shuttle vector carrying the *nisRK* genes and P*nisA* promoter	69
pORI280	*repA*-negative *lacZ*$^+$ derivative of pWV01	24, 25
pVE3916	Derivative of broad host range replicon pWV01	T. Rochat and P. Langella; Ref. 7
pVES3787	pVE3916 derivative carrying *pgdA* gene	7
pVE1837	pRV300 carrying 210-bp internal fragment of *ponA*	26
pLc-P40	pMSP3545 carrying *lcabl_00230* gene under nisin-inducible promoter	K. Regulski and M.-P. Chapot-Chartier, unpublished

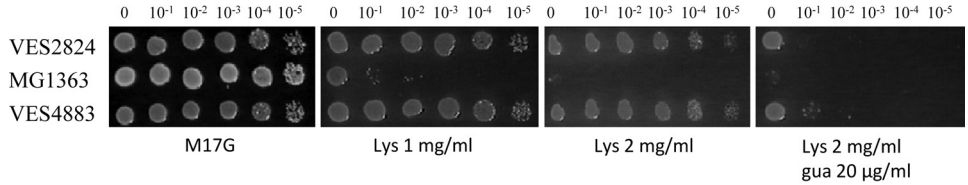

FIGURE 2. **Comparison of lysozyme resistance of *L. lactis* WT MG1363 and its mutants VES2824 in which a large region that included the *guaA* gene was deleted and VES4883 in which only the *guaA* gene was deleted.** Serially diluted cultures were grown on M17G agar plates supplemented with lysozyme (*Lys*) and guanine (*gua*).

Inactivation of pyrB Confers Lysozyme Resistance and Links Pyrimidine Biosynthesis to Peptidoglycan Assembly—The genes *pyrP*, *pyrR*, *pyrB*, and *carA*, which are strongly repressed in the Δ*guaA* mutant (Table 2), constitute an operon in *L. lactis* MG1363 (44). The *pyrP* gene encodes a uracil permease, which is required for utilization of exogenous uracil. The other two genes in the operon, *pyrB* and *carA*, encode pyrimidine biosynthetic enzymes. In *L. lactis*, PyrB is a unique aspartate transcarbamoylase that converts L-Asp to L-carbamoyl-L-aspartate (38). L-Asp is also used for CW biosynthesis: it is converted to D-Asp by RacD racemase and is subsequently attached to the stem peptide of PG by AslA ligase (10) and then converted to D-Asn by AsnH (9). Simultaneous utilization of L-Asp for PG and for pyrimidine biosynthesis could make the D-Asp/Asn content in the CW dependent on pyrimidine biosynthesis. In this case, *pyrB* could play a pivotal role in the tradeoff between L-Asp utilization for PG or for pyrimidine biosynthesis. Therefore we focused further studies on this gene by constructing a *pyrB* deletion mutant of MG1363 and testing this strain for lysozyme resistance.

Because the *L. lactis pyrB* mutant is a uracil auxotroph (38), the lysozyme resistance test was performed in M17G medium supplemented with uracil (100 μg/ml). We also included *L. lactis dltD* and *ponA* mutants because the expression of these genes was affected in the transcriptomics experiment described above (Table 2). We observed that a *ponA* mutation only slightly affected lysozyme resistance, whereas the inactivation of *dltD* in the Δ*guaA* mutant markedly abolished lysozyme resistance (Fig. 3). This indicates that increased teichoic acid alanylation may indeed play an important role in this phenotype of the Δ*guaA* mutant. Inactivation of *pyrB* resulted in lysozyme resistance; albeit it was slightly weaker than that of the Δ*guaA* mutant and of strain VES2824, which carried the large chromosomal deletion. Inactivation of *pyrB* in the Δ*guaA* mutant did not affect the lysozyme resistance phenotype, which was consistent with the transcriptomics data showing that *pyrB* is already strongly repressed in the Δ*guaA* mutant.

Inactivation of pyrB Results in a Thicker and More Rigid Cell Wall—The cell envelope of the Δ*pyrB* mutant growing exponentially in M17G medium was considerably thicker (41 ± 1.3

TABLE 2

Genes of VES4883 (ΔguaA) and of lysozyme-treated MG1363 that were up- and down-regulated compared with those in MG1363 (WT)

Only genes that were related to CW, involved in purine and pyrimidine metabolism, or whose expression was affected by more than 1.5-fold are indicated. Values indicate expression ratio (*n*-fold); values of down-regulated genes are in bold. lys, lysozyme; TCS, two-component system.

Locus	Gene	*guaA*	WT/lys	Function
PG synthesis				
llmg_0511	*ponA*	4.0		Penicillin-binding protein 1A
llmg_2316	*murC*	**−2.4**		UDP-*N*-acetylmuramate-L-alanine ligase
llmg_1329	*murB*	**−4.9**		UDP-*N*-acetylmuramate dehydrogenase
llmg_2165	*acmB*	2.8		*N*-Acetylmuramoyl-L-alanine amidase
Teichoic acid alanylation				
llmg_1220	*dltB*	3.4		Basic membrane protein
llmg_1219	*dltA*	3.3		D-Alanine-D-alanyl carrier protein ligase
llmg_1222	*dltD*	2.6		D-Alanine transfer protein
CesSR regulon				
llmg_1649	*cesS*		1.9	TCS sensor histidine kinase CesS
llmg_1648	*cesR*		1.9	TCS response regulator CesR
llmg_2164	*llmg_2164*		3.3	Predicted membrane protein
llmg_0165	*llmg_0165*		1.8	Predicted membrane protein
llmg_0169	*llmg_0169*		3.0	Predicted membrane protein
llmg_1155	*spxB*		3.1	Transcriptional regulator SpxB
llmg_1102	*llmg_1102*		1.5	Predicted membrane protein
llmg_1103	*llmg_1103*		1.9	Conserved hypothetical protein
Pyrimidine metabolism				
llmg_0890	*pyrR*	**−16.1**		Pyrimidine operon regulator PyrR
llmg_0891	*pyrP*	**−9.1**		Uracil permease
llmg_0893	*pyrB*	**−9.6**		Aspartate carbamoyltransferase
llmg_0894	*carA*	**−16.6**		Carbamoyl-phosphate synthase
llmg_0952	*pyrDA*	6.2		Dihydroorotate dehydrogenase
llmg_1105	*pyrK*	**−10.6**		Dihydroorotate dehydrogenase
llmg_1106	*pyrDB*	**−12.3**		Dihydroorotate dehydrogenase
llmg_1107	*pyrF*	**−20.8**		Orotidine-5′-phosphate decarboxylase
llmg_1508	*pyrC*	**−30.3**		Dihydroorotase
llmg_1509	*pyrE*	**−15.3**		Orotate phosphoribosyltransferase
Purine metabolism				
llmg_0230	*guaB*	9.5		Inositol-5-monophosphate dehydrogenase
llmg_0993	*hprT*	**−6.0**		Hypoxanthine phosphoribosyltransferase
llmg_1008	*guaA*	**−192.5**		GMP synthase
llmg_1412	*guaC*	**−17.9**		GMP reductase
llmg_2201	*purA*	**−4.4**	1.9	Adenylosuccinate synthetase

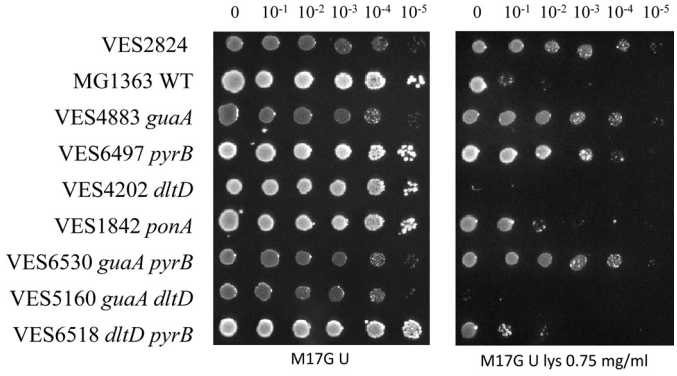

FIGURE 3. **Comparison of lysozyme resistance of the Δ*pyrB*, Δ*guaA*, *dltD*, and *ponA* mutants and the parental strain MG1363.** VES2824 is the spontaneous lysozyme-resistant mutant. The plate test was performed in M17G medium supplemented with 100 μg/ml uracil and lysozyme (*lys*).

nm; Fig. 4*B*) than that of parental strain MG1363 (36 ± 1.6 nm) as observed in transmission electron micrographs (Fig. 4*A*). Cell wall thickening was also observed in the Δ*pyrB* mutant when cells were grown in M17G supplemented with uracil (44 ± 2.6 *versus* 35 ± 1.7 nm for MG1363; Fig. 4*B*). As the transmission electron microscopy results pointed toward possible changes in cell wall rigidity in the Δ*pyrB* mutant, strains VES6497 (Δ*pyrB*) and MG1363 (WT) were grown in M17G medium with and without uracil (100 μg/ml) and examined by atomic force microscopy to measure cell wall rigidity (34, 45). Using an innovative method for sample immobilization in microstructured polydimethylsiloxane stamps (33) combined with multiparametric imaging, we were able to image *L. lactis* cells collected in the exponential growth phase while simultaneously probing their nanomechanical properties (rigidity of the cell wall). Height images (Fig. 5, *A*, *B*, *C*, and *D*) showed that the cell morphology was not modified by either *pyrB* inactivation or the addition of uracil to the culture medium. On the corresponding rigidity images (Fig. 5, *E*, *F*, *G*, and *H*), each pixel corresponds to a Young's modulus value, which reflects the rigidity of the cell wall. These images thus revealed that global stiffness varied between the two strains with darker MG1363 cells being softer than the lighter Δ*pyrB* mutants. However, two dividing cells did not always present the same nanomechanical properties (see Fig. 5*G*), which indicates that exponentially growing cells are heterogeneous in their cell wall rigidity. To precisely quantify the variations in cell stiffness, local force measurements were performed in small areas (500 × 500 nm) of the cells (46). Fig. 5*I* shows representative force *versus* indentation obtained from the two strains in the two growth conditions and fitted with a Hertz model to extract the Young's modulus values. As was already observed in the multiparametric imaging data, indentation curves (Fig. 5*I*) clearly show that MG1363 cells are softer than Δ*pyrB* mutant cells. Indeed, MG1363 cells display an average Young's modulus value that is 8-fold lower than that of Δ*pyrB* mutant cells both in the absence (226.9 ± 160.5 *versus* 1707.4 ± 920.4 kilopascals, respectively) and presence of uracil (95.8 ± 61.7 *versus* 780.1 ± 560.7 kilopascals,

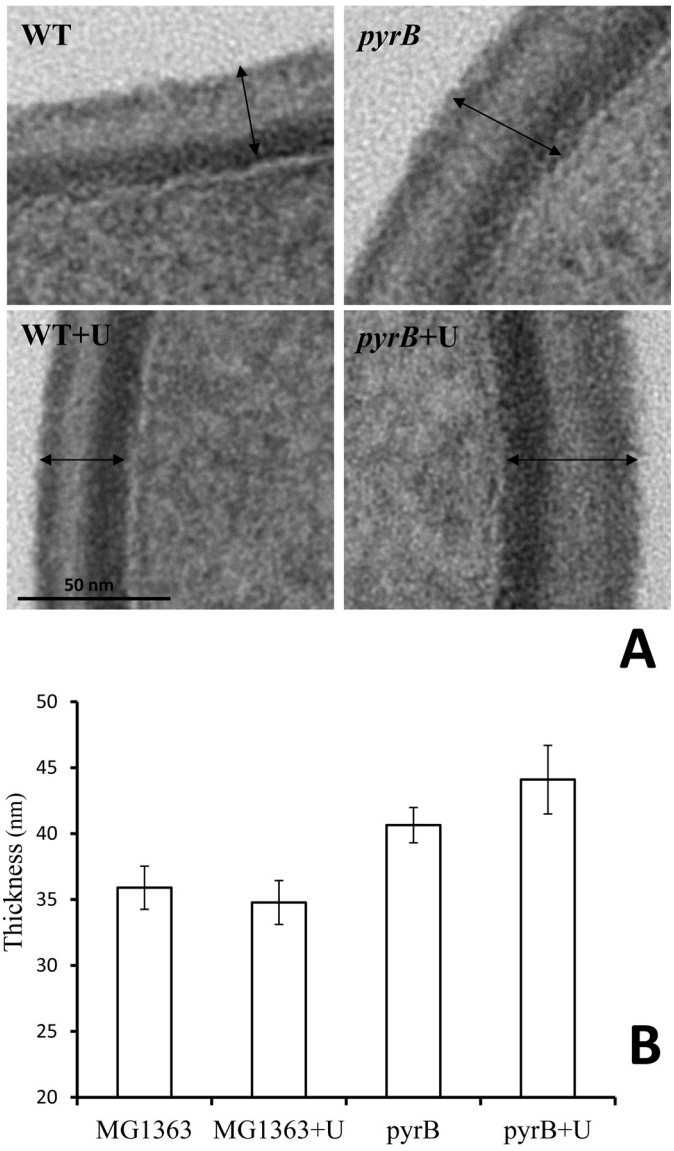

FIGURE 4. **Electron transmission micrographs (*A*) and evaluation of CW thickness (*B*) of *L. lactis* control strain MG1363 and its isogenic mutant VES6497 (Δ*pyrB*).** *Error bars* represent S.D. *Arrows* indicate the measured interval. *Scale bar*, 50 nm.

respectively) (Fig. 5*J*). Despite the large standard variations, which are due to the heterogeneity found in exponentially growing cells, the differences in Young's modulus values are highly significant ($p < 0.0001$). This quantitative analysis also showed that the presence of uracil resulted in an ~2-fold decrease in the rigidity of both wild type and mutant cells (Fig. 5*J*), which indicates that growth conditions have a slight impact on the nanomechanical properties of cell walls. Overall these nanomechanical data connected the increase in CW thickness in the Δ*pyrB* mutant that was observed in transmission electron microscopy with the rigidity of the cell wall; *i.e.* thicker cell walls are more rigid. Because it has been reported (7) that CW thickening is related to severe growth arrest of *L. lactis* cells, we further examined the growth characteristics of the Δ*pyrB* mutant.

Growth Defect of the ΔpyrB Mutant Is Linked to Cell Wall Rigidity—As reported previously (38), the Δ*pyrB* mutant was not able to grow in minimal SA medium without the addition of uracil (results not shown). Therefore we evaluated the growth characteristics of the Δ*pyrB* mutant in rich M17G medium. In this medium, the mutant exhibited a 5-h lag phase compared with its parent strain (Fig. 6*A*). This phenotype was complemented by introducing the positive allele of *pyrB* cloned in a plasmid under control of the nisin-inducible promoter. Note that in the medium without nisin partial complementation was observed in keeping with reports about the modest leakiness of this promoter (47). Interestingly, the growth delay was also restored by the addition of uracil to the medium, indicating that even in rich medium the Δ*pyrB* mutant is starved for nucleotides (Fig. 6). We further examined whether the growth impediment of the Δ*pyrB* mutant was due only to starvation for uracil or also to changes in the CW, possibly influencing its thickening and/or rigidity and consequently cell division and separation. To this end, we introduced into the Δ*pyrB* mutant a plasmid that carried a nisin-inducible gene encoding PGH Lc-P40 of *Lactobacillus casei*.[9] Lc-P40 (Lcabl_00230) is a PG-specific peptidase that hydrolyzes PG at the interpeptide bridges, which are formed by D-Asp in both *L. casei* and *L. lactis* (2, 48). We expected that Lc-P40 would "relax" the overly thick and rigid CW of the Δ*pyrB* mutant by creating breaks in PG. Indeed, the expression of Lc-P40 in the Δ*pyrB* mutant markedly increased growth, especially when the nisin inducer was added. It is important to note that the improvement in growth was observed in M17G medium without uracil, indicating that the growth delay of the Δ*pyrB* mutant was not only due to starvation for uracil.

Following the same reasoning, we mutated the *ponA* gene to create another "relaxation" factor in the Δ*pyrB* mutant. The *ponA* gene encodes PBP1A, an enzyme needed for the formation of PG cross-links, and mutations in it have been reported to favor the appearance of breaks in PG (15). As expected, the *ponA* mutation reduced the growth lag of the Δ*pyrB* mutant in M17G medium without uracil. Surprisingly, both "relaxing" genetic backgrounds (PGH-positive and *ponA*-negative) not only shortened the lag time but also increased the final OD of bacteria in the medium without uracil (Fig. 7).

We further examined how the growth of the Δ*pyrB* mutant was affected by certain factors that could reduce the number of PG breaks. For this, we introduced a multicopy plasmid that encoded the PG deacetylase gene *pgdA* in the Δ*pyrB* mutant. It was shown previously in *L. lactis* that this plasmid causes increased resistance to PG hydrolysis (6, 7), and for this reason we expected that overexpression of the $pgdA^+$ allele would increase the growth delay of the Δ*pyrB* mutant. Indeed, when the Δ*pyrB* mutant was grown in the presence of uracil, the introduction of multiple copies of $pgdA^+$ on a plasmid caused growth retardation (Fig. 8). In the WT strain, introduction of the same plasmid also caused growth delay but to a lesser extent.

We also examined *acmA*, the main lactococcal autolysin (14), as another factor that affects the number of breaks in PG (15). Deletion of *acmA* in the Δ*pyrB* mutant had a similar effect on growth delay, albeit less pronounced, as introduction of the

[9] K. Regulski and M.-P. Chapot-Chartier, personal communication.

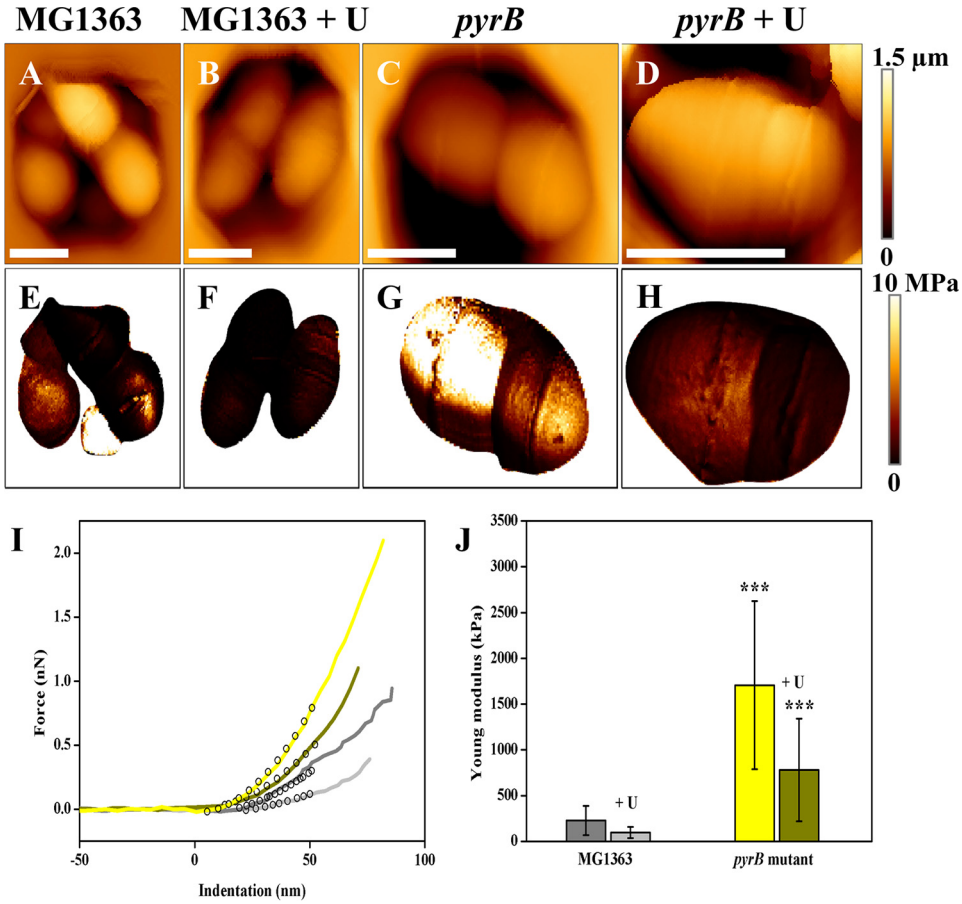

FIGURE 5. **Imaging and probing of the nanomechanical properties of living *L. lactis* cells.** Height images of cells of *L. lactis* MG1363 (*A*), MG1363 + uracil (100 μg/ml) (*B*), Δ*pyrB* mutant (*C*), and Δ*pyrB* mutant + uracil (100 μg/ml) (*D*), which were trapped in microstructured polydimethylsiloxane stamps (*scale bars* = 1 μm). *E*, *F*, *G*, and *H*, rigidity images corresponding to height images shown in *A*, *B*, *C*, and *D*, respectively. *I*, representative indentation curves obtained for MG1363 (*gray line*), MG1363 + uracil (*light gray line*), Δ*pyrB* mutant (*yellow line*), and Δ*pyrB* mutant + uracil (*dark yellow line*). *Black empty circles* show in each case the fit with the Hertz model. *J*, histogram showing the Young's modulus values for both strains with or without uracil. In each case, Young's modulus values were measured on 12 cells (n = 12,288 curves), and Young's modulus medians were calculated from fits in a Gaussian model. The *three asterisks* show significant differences between the rigidity of strain MG1363 and that of the Δ*pyrB* mutant at a p value <0.0001 (unpaired t test). *Error bars* represent S.D. *kPa*, kilopascals; *nN*, nanonewtons; *MPa*, megapascals.

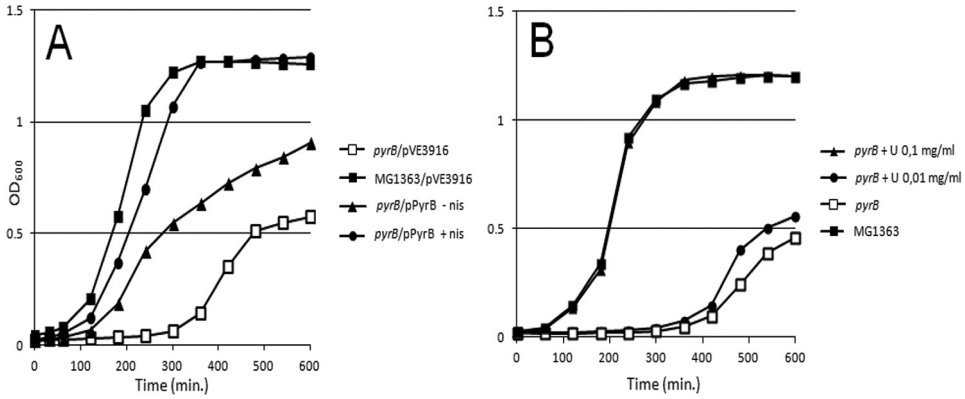

FIGURE 6. *A*, growth and complementation of the Δ*pyrB* mutant. *B*, complementation of growth of the Δ*pyrB* mutant by uracil. *nis*, nisin.

plasmid carrying *pgdA* did. Only a slight effect of the Δ*acmA* mutation was observable in the WT strain (Fig. 8*B*). Note that growth retardation caused by *pgdA* overexpression or by *acmA* deletion in the Δ*pyrB* mutant was seen in a medium with uracil, indicating that starvation for uracil is not responsible for the observed effects in the Δ*pyrB* mutant. In conclusion, the observed results are consistent with the increased CW rigidity of the Δ*pyrB* mutant compared with WT.

Inactivation of pyrB Increases D*-Asp/Asn-containing Muropeptides in PG and Cross-linking*—We determined the PG structure of exponentially growing *L. lactis* strains VES4883 (Δ*guaA*) and VES6497 (Δ*pyrB*) by separation of the constituent muropeptides by reverse phase HPLC and compared their muropeptide profiles with that of their parent, MG1363, which was grown to the exponential and early stationary phases. In keeping with the role of *pyrB* in the regulation of L-Asp avail-

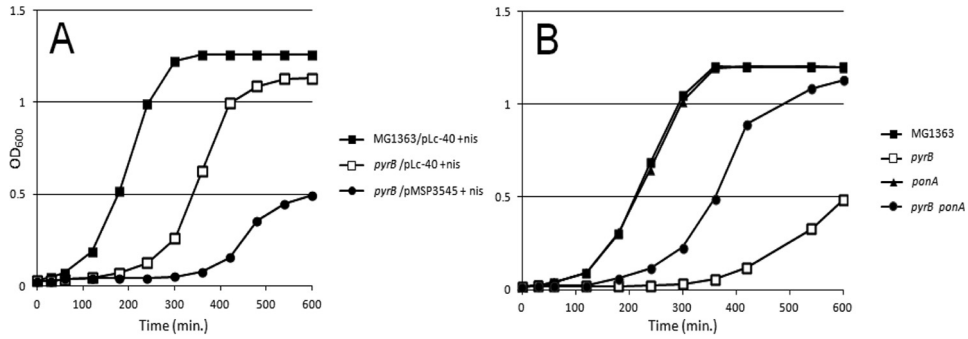

FIGURE 7. *A*, growth of MG1363 (WT) and a Δ*pyrB* mutant that carried a plasmid encoding *L. casei* BL23 PGH Lc-P40. *B*, growth of WT and a Δ*pyrB* mutant that carried a mutation in the *ponA* gene. Bacteria were grown in M17G medium without uracil. *nis*, nisin.

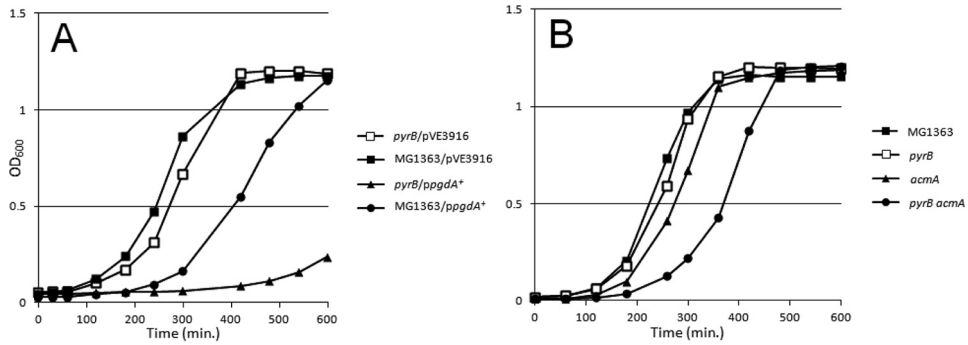

FIGURE 8. **Growth of MG1363 (WT) and Δ*pyrB* mutants carrying the *pgdA* gene of *L. lactis* on a multicopy plasmid (*A*) or deletion of the *acmA* gene (*B*) in M17G medium supplemented with uracil.**

ability for PG synthesis, more D-Asp/D-Asn was present in PG of both mutants (Table 3).

In particular, the reverse phase HPLC profiles of the Δ*guaA* and Δ*pyrB* mutants had fewer muropeptides that lacked D-Asp/Asn linked to their stem peptide (2.1 and 1.9%, respectively) relative to the control strain MG1363 in the same growth phase (4.0%). Furthermore, these two strains displayed elevated PG cross-linking (34.1 and 34.7%, respectively, *versus* 31.7% in WT). The MG1363 cells in early stationary phase (A_{600} 1.2) behaved similarly to Δ*pyrB* or Δ*guaA* mutants in the exponential growth phase (both at A_{600} 0.2). Among the muropeptides that contained D-Asp/Asn, a relative increase in D-Asn was seen in the CW of Δ*pyrB* or Δ*guaA* mutants and MG1363 in the early stationary phase: the Asn/Asp ratio in these strains was 3.1, 4.1, and 3.8, respectively, *versus* 2.2 for exponentially grown MG1363 (Table 3). Overall, the PG muropeptide analysis confirmed that there was more D-Asp/Asn in the PG of Δ*pyrB* and Δ*guaA* mutants, supporting the hypothesis that *pyrB* plays a pivotal role in the switch between L-Asp utilization for PG and its use in pyrimidine biosynthesis.

Discussion

The bacterial PG sacculus needs to be strong for cells to be able to withstand high turgor pressure. Rigid and thick PG is advantageous in the stationary phase when bacterial cells are exposed to different stress conditions, *e.g.* exhaustion and acidification of the medium (49). However, during exponential growth, PG must be flexible to allow fast cell division and enlargement. A balance between CW rigidity and flexibility may be maintained through the concerted activities of various enzymes involved in CW synthesis (PBPs) and hydrolysis (PGHs) (22, 50). Despite recent achievements in this field, the elucidation of the mechanisms that govern the maintenance of this balance remains a challenge. Notwithstanding extensive studies on bacterial PG modifications in response to PG hydrolysis-induced CW stress (51), little is known about the regulation of these processes under non-stress conditions.

Through the isolation of lysozyme-resistant mutants of *L. lactis* and the identification of the genes responsible for this phenotype, we were able to shed light on the mechanisms that govern the equilibrium between hydrolysis and synthesis of PG in this organism. Of the independent lysozyme-resistant isolates we obtained, 14% were guanine auxotrophs, which indicated that *guaA* was involved in the resistance phenotype. Whole-genome expression studies of the Δ*guaA* mutant showed decreased expression of the gene that encodes the regulator PyrR. This may be the reason why these mutants exhibited repression of the whole *pyr* operon (*pyrR*, *pyrP*, *pyrB*, and *carA*) and other genes involved in pyrimidine metabolism (44, 52). More studies are required to understand the precise regulatory mechanism that links the down-regulation of genes involved in pyrimidine metabolism with the inactivation of *guaA*. Because *guaA* is involved in the synthesis of guanosine monophosphate and consequently of the global regulatory alarmones (p)ppGpp (53), it might be that the latter participates in the regulatory scheme.

Most importantly, studies of the Δ*guaA* mutant led us to discover the contributions of *pyrB* to CW structure and properties. The aspartate carbamoyltransferase PyrB is responsible for the utilization of L-Asp for pyrimidine synthesis. L-Asp is

TABLE 3
Cross-linking index of PG and relative quantities of disaccharide building subunits in L. lactis MG1363 (WT), VES6497 (ΔpyrB), and VES4883 (ΔguaA)

	WT (A_{600} 0.5)	WT (A_{600} 1.2)	*pyrB* (A_{600} 0.2)	*guaA* (A_{600} 0.2)
PG cross-linking index	31.7	34.4	34.7	34.1
Sum[a] of disaccharide peptides without Asp/Asn (%)	4.0	3.5	1.9	2.1
Sum[a] of disaccharide peptides with Asp (%)	29.9	19.9	24.1	19.3
Sum[a] of disaccharide peptides with Asn (%)	66.1	76.5	74	78. 5
Ratio Asn/Asp	2.2	3.8	3.1	4.1

[a] The sum was calculated by considering disaccharide peptide building subunits constituting monomers, dimers, and trimers.

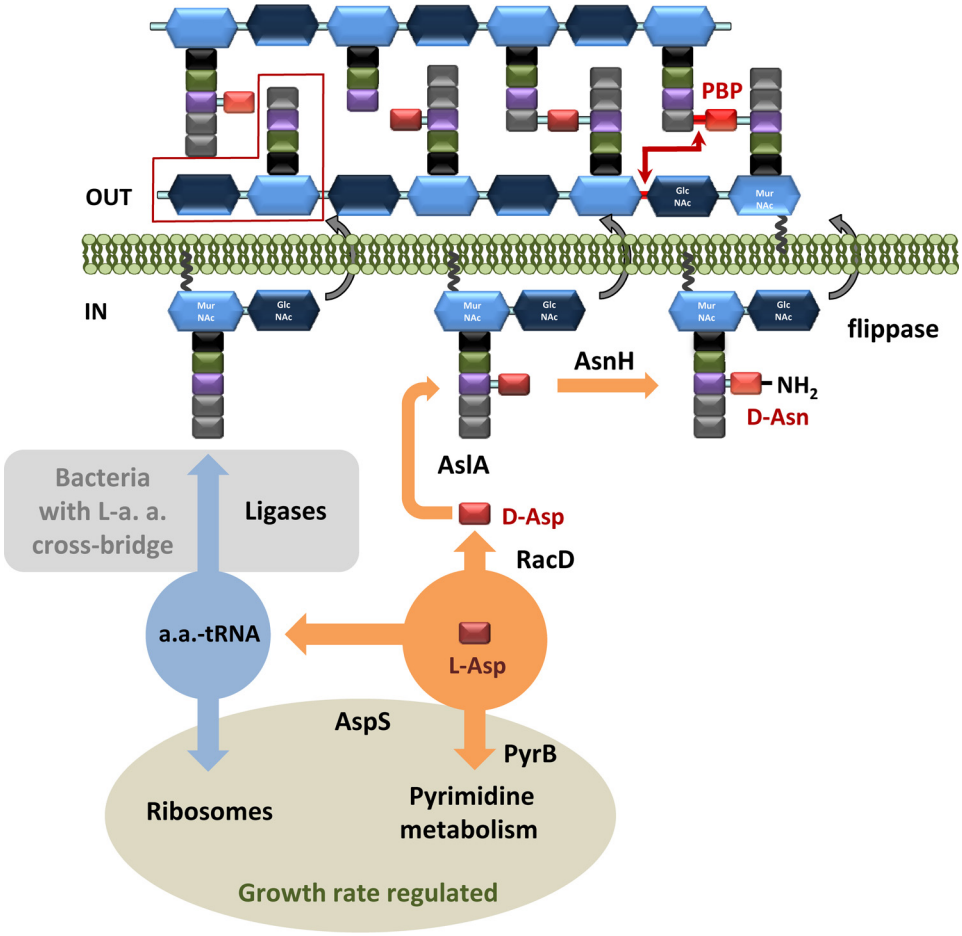

FIGURE 9. **Schematic representation of incorporation of D-Asp in *L. lactis* PG.** A representative D-Asp/Asp-less muropeptide is marked by a *red box*. Amino acids in PG stem peptides are presented as *squares*: *black*, L-Ala; *green*, D-Glu; *violet*, L-Lys; *red*, L- and D-Asp; *light red*, D-Asn. *N*-Acetylglucosamine is presented as a *blue hexagon*, and *N*-acetylmuramic acid is presented as a *light blue hexagon*. *a.a.*, aminoacyl; *L-a. a.*, L-amino acid.

also a precursor for CW synthesis (see Fig. 9): it is converted to D-Asp by racemase RacD, then attached to the stem peptide of the PG precursor by AslA ligase (10), and converted to D-Asn by AsnH (9). Simultaneous utilization of L-Asp for PG and for pyrimidine biosynthesis could provide the means of coordinating CW structure in a manner dependent on pyrimidine biosynthesis in which PyrB could play a pivotal role. We hypothesize that down-regulation of *pyrB* expression, as in the Δ*guaA* mutant, or its absence, as in the case of *pyrB* deletion, results in more L-Asp, which is transformed into D-Asp and used for the formation of PG cross-bridges. This would lead to the observed increase in PG rigidity and possibly to lysozyme resistance. To our knowledge, the data presented here indicate for the first time that a link exists between pyrimidine metabolism and CW plasticity in bacteria. This hypothesis is supported by the exceptional CW-related features of the Δ*pyrB* mutant: (i) the observed growth defects, which were restored by the introduction of additional mutations designed to weaken the CW (Figs. 6–8); (ii) increased PG cross-linking and D-Asp/D-Asn content (Table 3); (iii) elevated lysozyme resistance (Fig. 3); and (iv) increased CW thickness (Fig. 4) and rigidity (Fig. 5).

In particular, we observed a longer lag phase and lower final optical density in Δ*pyrB* mutant cultures than in the control strain MG1363 (Fig. 6). This growth defect was suppressed by introducing CW relaxing determinants in the Δ*pyrB* mutant, such as PGH of *L. casei* Lc-P40, which introduces breaks in PG interpeptide bridges, or a mutation in the *ponA* gene (Fig. 7). In addition, we exploited the fact that the growth defect was corrected by uracil to show that the opposite was also true, namely that the introduction of genetic factors that potentially lead to a

decrease in PG breaks resulted in growth retardation. Thus, overexpression of the PG deacetylase PgdA, which leads to resistance to autolysis and lysozyme through increased *N*-deacetylation of PG (6, 7), resulted in growth retardation in the Δ*pyrB* mutant. Removal of the main lactococcal autolysin AcmA (14) produced a similar, albeit less pronounced, effect.

Reverse phase HPLC analysis revealed that PG of the *pyrB*-negative strain as well as of the Δ*guaA* mutant (in which expression of *pyrB* was drastically decreased) contained fewer muropeptides that lacked D-Asp or D-Asn (1.9 and 2.1%, respectively) than the control strain (4.0%) in the exponential growth phase (Table 3). This was true regardless of whether the medium was supplemented or not with uracil (data not shown). The increased amount of D-Asp and D-Asn corresponds to an increased cross-linking index value (31.7% for WT *versus* 34.7 and 34.1% for Δ*pyrB* and Δ*guaA* mutants, respectively). Remarkably, the D-Asn/D-Asp ratios in PG of the Δ*pyrB* and the Δ*guaA* mutants were higher (3.1 and 4.1, respectively) than in the WT strain (2.2). Preferential accumulation of D-Asn in PG could be explained by the simultaneous increase in D-Asp supply in Δ*guaA* and Δ*pyrB* mutants, the activity of AsnH, and/or increased affinity of flippase for disaccharide pentapeptides carrying D-Asn. It has been reported that amidation of D-Asp renders *L. lactis* more resistant to lysozyme due to a decrease in the net negative charge of the CW (9). Therefore a higher amount of D-Asn in PG could result in a less negative CW charge, leading to elevated resistance to this cationic antimicrobial.

Interestingly, a relatively small increase in PG cross-linking and D-Asn/D-Asp content and ratio corresponded to considerable differences in other phenotypes, such as CW rigidity (Fig. 5), thickness (Fig. 4), growth defects (Fig. 7), and lysozyme resistance (Fig. 3). This might be explained by assuming that more intensively cross-linked PG is specifically localized, which, if true, would not have been observable in our experiments because of the sample-averaging nature of HPLC analyses (54). Similarly, it has been reported that a relatively moderate shift in PG *O*-acetylation (from 2.6 to 4.2%) caused complete growth arrest in *L. lactis* (7). The *pyrB* mutant phenotype could in part explain the high lysozyme resistance of the *guaA* mutant. The results presented here imply that the Δ*guaA* mutant possesses several regulatory mechanisms that enable it to prevent lysozyme activity, all potentially affecting cell envelope charge and/or PG cross-linking. First is the induction of the *dlt* operon, which is involved in alanylation of anionic teichoic acid (42, 55). The consequent decrease in negative charge of the CW increases resistance to the positively charged lysozyme (7). Second, an increase in the D-Asp/Asn supply due to *pyrB* down-regulation could result in elevated PG cross-linking and thus counteract the muramidase activity of lysozyme. Third, the presence of a higher amount of D-Asn in PG also results in a decrease in the net negative charge of the CW, which would increase lysozyme resistance. Moreover, the *ponA* gene, which encodes PBP 1A (26), was 4-fold overexpressed in the lysozyme-resistant Δ*guaA* mutant. It has been reported that up-regulation of PBP expression is a common strategy of Gram-positive bacteria responding to cell wall stress (51). Despite this, the *ponA* mutation did not increase the sensitivity of MG1363 to lysozyme activity (Fig. 3), suggesting that *ponA* overexpression only marginally affects this phenotype. Strikingly, the deletion of only one gene, namely *guaA*, protected against both types of lysozyme activities, the muramidase enzyme, and the cationic antibacterial peptide.

The link described here between *pyrB* expression and CW rigidity could have an important role in maintaining the balance between CW flexibility and rigidity during the growth of a bacterial community. This function is possible because the expression of pyrimidine metabolism genes is tightly linked to pyrimidine availability in the medium, which in turn depends on the growth phase of the culture (38, 44). Differential *pyrB* expression during culture growth was documented in chronotranscriptomics studies of *L. lactis* MG1363 grown in milk (56) or in M17G (57, 58). Notably, it was observed that the *pyr* operon is considerably more expressed during the exponential growth than it is in the stationary phase. If the D-Asp/D-Asn content in PG is dependent on *pyrB* expression, this would enable the availability of flexible PG during exponential growth and more rigid and thick PG in the stationary phase. In keeping with this reasoning, we observed a higher amount of Asp/Asn-less muropeptides in PG of MG1363 in the exponential phase than we did in the stationary phase. Correspondingly, the cross-linking index of MG1363 PG was lower in the exponential than in the stationary phase where it was comparable with that of the Δ*pyrB* mutant (Table 3).

Such "metabolic programming" would enable the maintenance of the needed CW plasticity without the need to transcriptionally control CW synthesis genes. It could be considered advantageous because the majority of CW synthesis genes are essential, and it has been suggested that essential genes in bacteria generally are not regulated at the transcriptional level (59). To avoid the transcriptional regulation of genes, encoding autolytic PGHs could also be advantageous because these are secreted extracellular enzymes, and thus their regulation via intracellular transcription could be challenging. In keeping with this interpretation, the lactococcal response to CW hydrolysis proceeds by modulating the target (*O*-acetylation of PG) rather than by decreasing transcription of the gene that codes for the secreted autolysin AcmA (7). Indeed, no decrease in expression of lactococcal PGH-encoding genes was observed in response to lysozyme treatment in our transcriptomics study (Table 2).

PG hydrolases are necessary for CW synthesis in growing cells (21, 60). The decrease of L-Asp availability in exponential phase, regulated by PyrB, leads to greater PG sensitivity to hydrolysis, which would be beneficial in terms of making PG more apt for incorporation of newly synthesized precursors.

The described hijacking of the regulatory circuit of pyrimidine metabolism, which is tightly regulated by growth requirements, to maintain an optimal balance between CW rigidity and flexibility may also take place in various other Gram-positive bacteria with D-Asp/D-Asn in their PG cross-bridges, such as *Enterococcus faecium*, *L. casei*, *Lactobacillus delbrueckii*, *Lactobacillus brevis*, and others (61). Interestingly, this mechanism is not used by *L. lactis* to respond to CW stress because *pyrB* is not down-regulated in cells treated with lysozyme (Table 2). It is probable that the tight regulation of genes

involved in nucleotide metabolism precludes the possibility of changing *pyrB* expression in response to CW stress.

This work shows that, to maintain optimal CW plasticity, bacteria regulate substrate availability (in this case L-Asp) for CW synthesis. The availability of L-Asp for CW synthesis might also be affected by expression of the aspartyl-tRNA synthetase gene *aspS*. This possibility is supported by the down-regulation of *aspS* in the stationary growth phase as observed in chrono-transcriptomics assays of *L. lactis* MG1363 grown in M17G (57, 58); this activity could also favor the availability of L-Asp for CW synthesis.

An analogous mechanism to the one described here might be at play in bacteria that have L-amino acids in their PG cross-bridges, such as *e.g. Streptococcus pneumoniae* (L-Ala-L-Ser or L-Ala-L-Ala in the cross-bridge). Like the competitive "switch" between PyrB and RacD for L-Asp and the resulting change in CW of *L. lactis*, in this case the competition between the protein synthesis machinery and tRNA-dependent aminoacyl ligases for aminoacylated-tRNA (62) could be a means of regulating PG plasticity. Ribosomal content is strictly regulated according to nutrient availability and is higher in the exponential phase than in the stationary phase (63). This would raise the probability of L-amino acids being incorporated in the PG cross-bridges of bacteria in stationary phase. The incorporation of amino acids in PG cross-bridges could therefore be viewed as an evolutionary adaptation enabling bacteria to tune PG plasticity to growth requirements.

Author Contributions—S. K. conceived and coordinated the study and wrote most of the paper. C. F.-D., P. H., and Y. F. D. designed, performed, and analyzed the atomic force microscopy experiments and wrote the corresponding part of the paper. C. P. designed, performed, and analyzed transmission electron microscopy experiments. A. S., O. P. K., and J. K. designed, performed, and analyzed the transcriptomics experiments and participated in the writing of the manuscript. P. C. and M.-P. C.-C. designed, performed, and analyzed the experiments shown in Table 2. S. F., P. V., and J. A. constructed strains. M. S. performed and analyzed the experiments shown in Figs. 6, 7, and 8. All authors reviewed the results and approved the final version of the manuscript.

Acknowledgments—We are indebted to A. Gruss, V. Fromion, and J. Martinussen for valuable discussions. We thank Carmen Bulbarela-Sampieri, Valerija Mikalaeva, Aurelie Bobillot, and Pascal Quenée for help in different phases of the work. The work of P. C., S. F., P. V., J. A., M. S., M.-P. C.-C., and S. K. benefited from the facilities and expertise of Microscopie et Imagerie des Micro-organismes, Animaux et Aliments Microscopie Électronique à Transmission, UMR 1313 Génétique Animale et Biologie Intégrative, Equipe Plateformes, Institut National de la Recherche Agronomique, Jouy-en-Josas, France.

References

1. Matsuhashi, M. (1994) Utilisation of lipid-linked precursors and the formation of peptidoglycan in the process of the cell growth and division: membrane enzymes involved in the final steps of peptidoglycan synthesis and the mechanism of their regulation, in *Bacterial Cell Wall* (Ghuysen, J. M., and Hakenbeck, R., eds) pp. 55–71, Elsevier, Amsterdam
2. Chapot-Chartier, M. P., and Kulakauskas, S. (2014) Cell wall structure and function in lactic acid bacteria. *Microb. Cell Fact.* **13,** Suppl. 1, S9
3. Loskill, P., Pereira, P. M., Jung, P., Bischoff, M., Herrmann, M., Pinho, M. G., and Jacobs, K. (2014) Reduction of the peptidoglycan crosslinking causes a decrease in stiffness of the *Staphylococcus aureus* cell envelope. *Biophys. J.* **107,** 1082–1089
4. Vollmer, W. (2008) Structural variation in the glycan strands of bacterial peptidoglycan. *FEMS Microbiol. Rev.* **32,** 287–306
5. Moynihan, P. J., and Clarke, A. J. (2011) O-Acetylated peptidoglycan: controlling the activity of bacterial autolysins and lytic enzymes of innate immune systems. *Int. J. Biochem. Cell Biol.* **43,** 1655–1659
6. Meyrand, M., Boughammoura, A., Courtin, P., Mézange, C., Guillot, A., and Chapot-Chartier, M. P. (2007) Peptidoglycan N-acetylglucosamine deacetylation decreases autolysis in *Lactococcus lactis*. *Microbiology* **153,** 3275–3285
7. Veiga, P., Bulbarela-Sampieri, C., Furlan, S., Maisons, A., Chapot-Chartier, M. P., Erkelenz, M., Mervelet, P., Noirot, P., Frees, D., Kuipers, O. P., Kok, J., Gruss, A., Buist, G., and Kulakauskas, S. (2007) SpxB regulates *O*-acetylation-dependent resistance of *Lactococcus lactis* peptidoglycan to hydrolysis. *J. Biol. Chem.* **282,** 19342–19354
8. van Heijenoort, J. (2007) Lipid intermediates in the biosynthesis of bacterial peptidoglycan. *Microbiol. Mol. Biol. Rev.* **71,** 620–635
9. Veiga, P., Erkelenz, M., Bernard, E., Courtin, P., Kulakauskas, S., and Chapot-Chartier, M. P. (2009) Identification of the asparagine synthase responsible for D-Asp amidation in the *Lactococcus lactis* peptidoglycan interpeptide crossbridge. *J. Bacteriol.* **191,** 3752–3757
10. Veiga, P., Piquet, S., Maisons, A., Furlan, S., Courtin, P., Chapot-Chartier, M. P., and Kulakauskas, S. (2006) Identification of an essential gene responsible for D-Asp incorporation in the *Lactococcus lactis* peptidoglycan crossbridge. *Mol. Microbiol.* **62,** 1713–1724
11. Chapot-Chartier, M. P. (2010) Bacterial autolysins, in *Prokaryotic Cell Wall Compounds* (König, H., Claus, H., and Varma, A. eds) pp. 383–406, Springer Verlag, Heidelberg, Germany
12. Vollmer, W., Joris, B., Charlier, P., and Foster, S. (2008) Bacterial peptidoglycan (murein) hydrolases. *FEMS Microbiol. Rev.* **32,** 259–286
13. Lee, T. K., and Huang, K. C. (2013) The role of hydrolases in bacterial cell-wall growth. *Curr. Opin. Microbiol.* **16,** 760–766
14. Buist, G., Kok, J., Leenhouts, K. J., Dabrowska, M., Venema, G., and Haandrikman, A. J. (1995) Molecular cloning and nucleotide sequence of the gene encoding the major peptidoglycan hydrolase of *Lactococcus lactis*, a muramidase needed for cell separation. *J. Bacteriol.* **177,** 1554–1563
15. Mercier, C., Domakova, E., Tremblay, J., and Kulakauskas, S. (2000) Effects of a muramidase on a mixed bacterial community. *FEMS Microbiol. Lett.* **187,** 47–52
16. Cava, F., and de Pedro, M. A. (2014) Peptidoglycan plasticity in bacteria: emerging variability of the murein sacculus and their associated biological functions. *Curr. Opin. Microbiol.* **18,** 46–53
17. Buckley, N. D., Vadeboncoeur, C., LeBlanc, D. J., Lee, L. N., and Frenette, M. (1999) An effective strategy, applicable to *Streptococcus salivarius* and related bacteria, to enhance or confer electroporation competence. *Appl. Environ. Microbiol.* **65,** 3800–3804
18. Cruz-Rodz, A. L., and Gilmore, M. S. (1990) High efficiency introduction of plasmid DNA into glycine treated *Enterococcus faecalis* by electroporation. *Mol. Gen. Genet.* **224,** 152–154
19. Bisicchia, P., Noone, D., Lioliou, E., Howell, A., Quigley, S., Jensen, T., Jarmer, H., and Devine, K. M. (2007) The essential YycFG two-component system controls cell wall metabolism in *Bacillus subtilis*. *Mol. Microbiol.* **65,** 180–200
20. Singh, S. K., SaiSree, L., Amrutha, R. N., and Reddy, M. (2012) Three redundant murein endopeptidases catalyse an essential cleavage step in peptidoglycan synthesis of *Escherichia coli* K12. *Mol. Microbiol.* **86,** 1036–1051
21. Vollmer, W. (2012) Bacterial growth does require peptidoglycan hydrolases. *Mol. Microbiol.* **86,** 1031–1035
22. Wheeler, R., Turner, R. D., Bailey, R. G., Salamaga, B., Mesnage, S., Mohamad, S. A., Hayhurst, E. J., Horsburgh, M., Hobbs, J. K., and Foster, S. J. (2015) Bacterial cell enlargement requires control of cell wall stiffness mediated by peptidoglycan hydrolases. *MBio* **6,** e00660
23. Gasson, M. J. (1983) Plasmid complements of *Streptococcus lactis* NCDO

712 and other lactic streptococci after protoplast-induced curing. *J. Bacteriol.* **154,** 1–9
24. Law, J., Buist, G., Haandrikman, A., Kok, J., Venema, G., and Leenhouts, K. (1995) A system to generate chromosomal mutations in *Lactococcus lactis* which allows fast analysis of targeted genes. *J. Bacteriol.* **177,** 7011–7018
25. Leenhouts, K., Buist, G., Bolhuis, A., ten Berge, A., Kiel, J., Mierau, I., Dabrowska, M., Venema, G., and Kok, J. (1996) A general system for generating unlabelled gene replacements in bacterial chromosomes. *Mol. Gen. Genet.* **253,** 217–224
26. Mercier, C., Durrieu, C., Briandet, R., Domakova, E., Tremblay, J., Buist, G., and Kulakauskas, S. (2002) Positive role of peptidoglycan breaks in lactococcal biofilm formation. *Mol. Microbiol.* **46,** 235–243
27. Gibson, D. G., Young, L., Chuang, R. Y., Venter, J. C., Hutchison, C. A., 3rd, and Smith, H. O. (2009) Enzymatic assembly of DNA molecules up to several hundred kilobases. *Nat. Methods* **6,** 343–345
28. Courtin, P., Miranda, G., Guillot, A., Wessner, F., Mézange, C., Domakova, E., Kulakauskas, S., and Chapot-Chartier, M. P. (2006) Peptidoglycan structure analysis of *Lactococcus lactis* reveals the presence of an L,D-carboxypeptidase involved in peptidoglycan maturation. *J. Bacteriol.* **188,** 5293–5298
29. Regulski, K., Courtin, P., Kulakauskas, S., and Chapot-Chartier, M. P. (2013) A novel type of peptidoglycan-binding domain highly specific for amidated D-Asp cross-bridge, identified in *Lactobacillus casei* bacteriophage endolysins. *J. Biol. Chem.* **288,** 20416–20426
30. Glauner, B. (1988) Separation and quantification of muropeptides with high-performance liquid chromatography. *Anal. Biochem.* **172,** 451–464
31. van Hijum, S. A., de Jong, A., Baerends, R. J., Karsens, H. A., Kramer, N. E., Larsen, R., den Hengst, C. D., Albers, C. J., Kok, J., and Kuipers, O. P. (2005) A generally applicable validation scheme for the assessment of factors involved in reproducibility and quality of DNA-microarray data. *BMC Genomics* **6,** 77
32. Zomer, A. L., Buist, G., Larsen, R., Kok, J., and Kuipers, O. P. (2007) Time-resolved determination of the CcpA regulon of *Lactococcus lactis* spp. cremoris MG1363. *J. Bacteriol.* **189,** 1366–1381
33. Formosa, C., Pillet, F., Schiavone, M., Duval, R. E., Ressier, L., and Dague, E. (2015) Generation of living cell arrays for atomic force microscopy studies. *Nat. Protoc.* **10,** 199–204
34. Chopinet, L., Formosa, C., Rols, M. P., Duval, R. E., and Dague, E. (2013) Imaging living cells surface and quantifying its properties at high resolution using AFM in QI mode. *Micron* **48,** 26–33
35. Hutter, J. L., and Bechhoefer, J. (1993) Calibration of atomic-force microscope tips. *Rev. Sci. Instrum.* **64,** 1868–1873
36. Ibrahim, H. R., Thomas, U., and Pellegrini, A. (2001) A helix-loop-helix peptide at the upper lip of the active site cleft of lysozyme confers potent antimicrobial activity with membrane permeabilization action. *J. Biol. Chem.* **276,** 43767–43774
37. Jensen, P. R., and Hammer, K. (1993) Minimal requirements for exponential growth of *Lactococcus lactis*. *Appl. Environ. Microbiol.* **59,** 4363–4366
38. Kilstrup, M., Hammer, K., Ruhdal Jensen, P., and Martinussen, J. (2005) Nucleotide metabolism and its control in lactic acid bacteria. *FEMS Microbiol. Rev.* **29,** 555–590
39. Rallu, F., Gruss, A., Ehrlich, S. D., and Maguin, E. (2000) Acid- and multi-stress-resistant mutants of *Lactococcus lactis*: identification of intracellular stress signals. *Mol. Microbiol.* **35,** 517–528
40. Wegmann, U., O'Connell-Motherway, M., Zomer, A., Buist, G., Shearman, C., Canchaya, C., Ventura, M., Goesmann, A., Gasson, M. J., Kuipers, O. P., van Sinderen, D., and Kok, J. (2007) Complete genome sequence of the prototype lactic acid bacterium *Lactococcus lactis* subsp. cremoris MG1363. *J. Bacteriol.* **189,** 3256–3270
41. Daveran-Mingot, M. L., Campo, N., Ritzenthaler, P., and Le Bourgeois, P. (1998) A natural large chromosomal inversion in *Lactococcus lactis* is mediated by homologous recombination between two insertion sequences. *J. Bacteriol.* **180,** 4834–4842
42. Reichmann, N. T., Cassona, C. P., and Gründling, A. (2013) Revised mechanism of D-alanine incorporation into cell wall polymers in Gram-positive bacteria. *Microbiology* **159,** 1868–1877
43. Martínez, B., Zomer, A. L., Rodríguez, A., Kok, J., and Kuipers, O. P. (2007) Cell envelope stress induced by the bacteriocin Lcn972 is sensed by the lactococcal two-component system CesSR. *Mol. Microbiol.* **64,** 473–486
44. Martinussen, J., Schallert, J., Andersen, B., and Hammer, K. (2001) The pyrimidine operon pyrRPB-carA from *Lactococcus lactis*. *J. Bacteriol.* **183,** 2785–2794
45. Dufrêne, Y. F. (2014) Atomic force microscopy in microbiology: new structural and functional insights into the microbial cell surface. *MBio* **5,** e01363–01314
46. Touhami, A., Nysten, B., and Dufrene, Y. F. (2003) Nanoscale mapping of the elasticity of microbial cells by atomic force microscopy. *Langmuir* **19,** 4539–4543
47. Renye, J. A., Jr., and Somkuti, G. A. (2010) Nisin-induced expression of pediocin in dairy lactic acid bacteria. *J. Appl. Microbiol.* **108,** 2142–2151
48. Regulski, K., Courtin, P., Meyrand, M., Claes, I. J., Lebeer, S., Vanderleyden, J., Hols, P., Guillot, A., and Chapot-Chartier, M. P. (2012) Analysis of the peptidoglycan hydrolase complement of *Lactobacillus casei* and characterization of the major γ-D-glutamyl-L-lysyl-endopeptidase. *PLoS One* **7,** e32301
49. Rallu, F., Gruss, A., and Maguin, E. (1996) *Lactococcus lactis* and stress. *Antonie Van Leeuwenhoek* **70,** 243–251
50. Pinho, M. G., Kjos, M., and Veening, J. W. (2013) How to get (a)round: mechanisms controlling growth and division of coccoid bacteria. *Nat. Rev. Microbiol.* **11,** 601–614
51. Jordan, S., Hutchings, M. I., and Mascher, T. (2008) Cell envelope stress response in Gram-positive bacteria. *FEMS Microbiol. Rev.* **32,** 107–146
52. Martinussen, J., Andersen, P. S., and Hammer, K. (1994) Nucleotide metabolism in *Lactococcus lactis*: salvage pathways of exogenous pyrimidines. *J. Bacteriol.* **176,** 1514–1516
53. Hauryliuk, V., Atkinson, G. C., Murakami, K. S., Tenson, T., and Gerdes, K. (2015) Recent functional insights into the role of (p)ppGpp in bacterial physiology. *Nat. Rev. Microbiol.* **13,** 298–309
54. Turner, R. D., Vollmer, W., and Foster, S. J. (2014) Different walls for rods and balls: the diversity of peptidoglycan. *Mol. Microbiol.* **91,** 862–874
55. Steen, A., Palumbo, E., Deghorain, M., Cocconcelli, P. S., Delcour, J., Kuipers, O. P., Kok, J., Buist, G., and Hols, P. (2005) Autolysis of *Lactococcus lactis* is increased upon D-alanine depletion of peptidoglycan and lipoteichoic acids. *J. Bacteriol.* **187,** 114–124
56. de Jong, A., Hansen, M. E., Kuipers, O. P., Kilstrup, M., and Kok, J. (2013) The transcriptional and gene regulatory network of *Lactococcus lactis* MG1363 during growth in milk. *PLoS One* **8,** e53085
57. Brouwer, R. W. W. (2014) *Computational Methods for the Analysis of Bacterial Gene Regulation*, Ph.D. thesis, University of Groningen, The Netherlands
58. Pinto, J. (2015) *In Principio erat Lactococcus lactis: towards a Membrane Protein Overproducer Host*, Ph.D. thesis, University of Groningen, The Netherlands
59. Kobayashi, K., Ehrlich, S. D., Albertini, A., Amati, G., Andersen, K. K., Arnaud, M., Asai, K., Ashikaga, S., Aymerich, S., Bessieres, P., Boland, F., Brignell, S. C., Bron, S., Bunai, K., Chapuis, J., *et al.* (2003) Essential *Bacillus subtilis* genes. *Proc. Natl. Acad. Sci. U.S.A.* **100,** 4678–4683
60. Vollmer, W., and Höltje, J. V. (2004) The architecture of the murein (peptidoglycan) in Gram-negative bacteria: vertical scaffold or horizontal layer(s)? *J. Bacteriol.* **186,** 5978–5987
61. Schleifer, K. H., and Kandler, O. (1972) Peptidoglycan types of bacterial cell walls and their taxonomic implications. *Bacteriol. Rev.* **36,** 407–477
62. Shepherd, J., and Ibba, M. (2013) Direction of aminoacylated transfer RNAs into antibiotic synthesis and peptidoglycan-mediated antibiotic resistance. *FEBS Lett.* **587,** 2895–2904
63. Wilson, D. N., and Nierhaus, K. H. (2007) The weird and wonderful world of bacterial ribosome regulation. *Crit. Rev. Biochem. Mol. Biol.* **42,** 187–219
64. Kuipers, O. P., de Ruyter, P., Kleerebezem, M., and de Vos, W. M. (1998) Quorum sensing-controlled gene expression in lactic acid bacteria. *J. Biotechnol.* **64,** 15–21

65. Duwat, P., Cochu, A., Ehrlich, S. D., and Gruss, A. (1997) Characterization of *Lactococcus lactis* UV-sensitive mutants obtained by ISS1 transposition. *J. Bacteriol.* **179,** 4473–4479
66. Boyer, H. W., and Roulland-Dussoix, D. (1969) A complementation analysis of the restriction and modification of DNA in *Escherichia coli*. *J. Mol. Biol.* **41,** 459–472
67. Leloup, L., Ehrlich, S. D., Zagorec, M., and Morel-Deville, F. (1997) Single-crossover integration in the *Lactobacillus sake* chromosome and insertional inactivation of the ptsI and lacL genes. *Appl. Environ. Microbiol.* **63,** 2117–2123
68. Maguin, E., Duwat, P., Hege, T., Ehrlich, D., and Gruss, A. (1992) New thermosensitive plasmid for Gram-positive bacteria. *J. Bacteriol.* **174,** 5633–5638
69. Bryan, E. M., Bae, T., Kleerebezem, M., and Dunny, G. M. (2000) Improved vectors for nisin-controlled expression in Gram-positive bacteria. *Plasmid* **44,** 183–190